ARMY RESEARCH LABORATORY

Urban-Small Building Complex Environment: *W07US* Stability Analysis, Volume AS-3 (Urban Versus Rural Diurnal Stability Cycles)

by Gail Vaucher

ARL-TR-4954   **September 2009**

NOTICES

Disclaimers

The findings in this report are not to be construed as an official Department of the Army position unless so designated by other authorized documents.

Citation of manufacturer's or trade names does not constitute an official endorsement or approval of the use thereof.

Destroy this report when it is no longer needed. Do not return it to the originator.

Army Research Laboratory

White Sands Missile Range, NM 88002-5513

Urban-Small Building Complex Environment: *W07US* Stability Analysis, Volume AS-3 (Urban Versus Rural Diurnal Stability Cycles)

Gail Vaucher
Computational Information Sciences Directorate, ARL

REPORT DOCUMENTATION PAGE		*Form Approved* *OMB No. 0704-0188*

REPORT DOCUMENTATION PAGE

Form Approved
OMB No. 0704-0188

Public reporting burden for this collection of information is estimated to average 1 hour per response, including the time for reviewing instructions, searching existing data sources, gathering and maintaining the data needed, and completing and reviewing the collection information. Send comments regarding this burden estimate or any other aspect of this collection of information, including suggestions for reducing the burden, to Department of Defense, Washington Headquarters Services, Directorate for Information Operations and Reports (0704-0188), 1215 Jefferson Davis Highway, Suite 1204, Arlington, VA 22202-4302. Respondents should be aware that notwithstanding any other provision of law, no person shall be subject to any penalty for failing to comply with a collection of information if it does not display a currently valid OMB control number.
PLEASE DO NOT RETURN YOUR FORM TO THE ABOVE ADDRESS.

1. REPORT DATE *(DD-MM-YYYY)* September 2009	2. REPORT TYPE Final	3. DATES COVERED (From - To)
4. TITLE AND SUBTITLE Urban-Small Building Complex Environment: *W07US* Stability Analysis, Volume AS-3 (Urban Versus Rural Diurnal Stability Cycles)		5a. CONTRACT NUMBER
		5b. GRANT NUMBER
		5c. PROGRAM ELEMENT NUMBER
6. AUTHOR(S) Gail Vaucher		5d. PROJECT NUMBER
		5e. TASK NUMBER
		5f. WORK UNIT NUMBER
7. PERFORMING ORGANIZATION NAME(S) AND ADDRESS(ES) U.S. Army Research Laboratory Computational and Information Sciences Directorate Battlefield Environment Division (ATTN: RDRL-CIE-D) White Sands Missile Range, NM 88002-5501		8. PERFORMING ORGANIZATION REPORT NUMBER ARL-TR-4954
9. SPONSORING/MONITORING AGENCY NAME(S) AND ADDRESS(ES)		10. SPONSOR/MONITOR'S ACRONYM(S)
		11. SPONSOR/MONITOR'S REPORT NUMBER(S)
12. DISTRIBUTION/AVAILABILITY STATEMENT Approved for public release; distribution is unlimited.		
13. SUPPLEMENTARY NOTES		

14. ABSTRACT

This report documents the urban diurnal stability cycle research, an outgrowth of the ongoing Urban Stability research begun with the WSMR 2003 Urban Study field project. The long term goal for this investigation is to develop an empirical Neutral Event Forecast Model for the urban environment. This quest stems from the success of a Neutral Event Forecast Model which was created for an operational high energy laser test facility located in a rural desert environment. Neutral events represent periods during which the atmosphere have a minimal impact on the laser operation; thus, they have a significant impact on the site mission. This report gives a background of stability from two perspectives, discusses the character of the urban stable conditions observed in the supporting datasets of this study, describes the rural and urban diurnal stability cycles, and finally presents qualitative equations for predicting the urban and rural diurnal stability cycle anchors known as the "neutral events."

15. SUBJECT TERMS

Urban, stability cycles, stable urban conditions, neutral events, Neutral Event Forecast Model, *W03US*, *W05US*, *W07US*.

16. SECURITY CLASSIFICATION OF:			17. LIMITATION OF ABSTRACT	18. NUMBER OF PAGES	19a. NAME OF RESPONSIBLE PERSON Gail Vaucher
a. REPORT Unclassified	b. ABSTRACT Unclassified	c. THIS PAGE Unclassified	UU	44	19b. TELEPHONE NUMBER *(Include area code)* (575) 678-3237

Contents

List of Figures

List of Tables

Executive Summary

This report documents the urban diurnal stability cycle research, an outgrowth of the ongoing Urban Stability research begun with the *White Sands Missile Range (WSMR) 2003 Urban Study* (*W03US*) field project. The long term goal for this investigation is to develop an empirical Neutral Event (NE) Forecast Model for the urban environment. This quest stems from the success of an NE Forecast Model which was created for an operational high energy laser test facility located in a rural desert environment. Neutral Events represent periods during which the atmosphere had a minimal impact on the laser operation; thus, they had a significant impact on the site mission. This report gives a background of stability from two perspectives, discusses the character of the urban stable conditions observed in the supporting datasets of this study, describes the rural and urban diurnal stability cycles, and finally presents qualitative equations for predicting the rural and urban diurnal stability cycle anchors, called "the neutral events."

There are at least two methods for understanding atmospheric stability: the classical micro-meteorological approach and the electro-optical propagation applications approach. The classical micro-meteorological approach examines stability through vertical temperature gradients (lapse rates) and micro-meteorological turbulence parameters. The electro-optical propagation applications approach examines stability through atmospheric density variations along a path and atmospheric optical turbulence parameters. The tools used in this urban diurnal stability cycle research utilized both perspectives.

Three urban field studies were conducted by the U.S. Army Research Laboratory (ARL) around a single, two-story urban building in a small building complex in southern New Mexico. These studies investigated both the urban stability and wind flow patterns. Based on this dataset, three general urban stability patterns were identified: the Always Unstable (1-state stability) cycle, the Unstable and Neutral (2-state stability) cycle, and the Unstable, Neutral and Stable (3-state stability) cycle. Examples of each will be presented in this report.

Stable atmospheric conditions are not normally associated with an urban environment. Therefore, a closer look into the character of this stable state was pursued. Drawing from the three urban field studies, temporal and spatial attributes for this unexpected urban stable state were identified.

With the stable state better understood, the single rural and three urban diurnal stability cycles were re-examined. The neutral condition was the key element in creating the rural NE Forecast Model. Two urban patterns contained neutral conditions. Each showed a different function for the neutral status. In the Unstable and Neutral, the time-extended neutral condition seemed to loiter before returning to an unstable state. In the 3-state stability cycle, the neutral environment served as a transition between stability states. The NE relevant to this study were defined as

those periods in which the atmosphere transitions between stable and unstable (and visa versa) conditions. Therefore, the time-extended neutral environment of the two-state urban cycle was deemed important, but secondary, to the transitory neutral event function of the three-state urban cycle. Focusing on this three-state cycle and the transitory neutral events, the gross diurnal pattern appeared to be nearly identical to the rural stability cycle. Examining the urban cycle as a function of which side of the building was being studied, there were several distinguishing attributes.

An example from the *WSMR 2007 Urban Study* (*W07US)* dataset was used to demonstrate the morning and evening NE character for each side of the building. The abrupt nature of the morning NE and the gradual transition in the evening NE imitated the rural time series data collected within 30 miles of the site. Therefore, this pattern was identified as being a function of the common (rural and urban) eastern and western horizons. The temporal order in which the building sides reported a NE transition seemed to be a function of several factors. The four identified were "solar angle," "systematic shadowing," "site-specific shadowing," and the "greatest local anthropological influence." The top two influences for the urban NE Forecast Model were also the top two factors for the rural NE Forecast Model. That is, the "solar angle" (sunrise/sunset time of day) adjusted for season and, the "systematic shadowing" or, cloud effects. The "site specific shadowing" was due to structural resources such as buildings, trees, fences, etc. This influence was a factor for the rural model too; however, since the field tests from which the model was created were conducted over a relatively-flat, open, desert terrain, the effects were not significant. The "greatest local anthropological influence" consisted of items such as the subject building's or neighboring building's heat. This heat could take the form of infrared radiation or vented exhaust. Ground moisture was a foundational influence for the rural NE Model. However, due to the efficient water management in urban areas, this contribution was not considered a significant factor.

This report concludes that, based on the study discussed, the Rural and Urban NE Models could be summarized as follows:

Rural Neutral Event Forecast Model
NE = Solar Angle + Systematic Shadowing + Ground Moisture

Urban Neutral Event Forecast Model
NE = Solar Angle + Systematic Shadowing + Site-specific Shadowing
+ the Greatest Local Anthropological Influence

In future research studies, the qualitative urban stability cycle equation(s) will be converted into mathematical representations and tested against the existing datasets. Due to the complexity of the urban environment, these equations will likely consist of both empirical observations and basic physical principles.

1. Background

Atmospheric stability cycles impact where we live, grow our food, and how we conduct our business. Examples of stability applications include the transport and dispersion of air pollutants or hazardous chemicals, convective cloud development which can lead to beneficial rain or to severe storms, and atmospheric optical propagation such as high energy laser transmissions through the open air.

Stability patterns are driven by several atmospheric phenomena including advection, subsidence and the ambient radiative heating and cooling cycles. While stability cycles occur at various levels in the atmosphere, the most easily discerned cycle occurs near the ground, in a shallow layer of the troposphere called the "Boundary Layer." The Boundary Layer generally covers an area from the surface, up to about 1 to 2 km. The lowest 10% of this Boundary Layer is called the "Surface Layer." This sub-layer is often characterized by its radiative heating and cooling attributes or stability, and is the context for this research.

1.1   Atmospheric Stability

Atmospheric stability is defined as the resistance of the atmosphere to vertical motion (Jenkins, 2009) or a condition of buoyancy within the atmosphere. Stability that considers only buoyancy is called "static stability." Dynamic stability considers both buoyancy and the shear in the mean wind. In this report, we will consider static stability, unless otherwise indicated.

To determine the type of static stability, one first presumes that the atmosphere is in a hydrostatic equilibrium. A comparison between an air parcel and its surrounding environment then determines the stability type (Glickman, 2000). There are three general stability types:

1. UNSTABLE Static Stability: If an air parcel is warmer than its surroundings at the same height or pressure, the parcel is positively buoyant and, if given an initial motion, will rise until it reaches equilibrium with its surroundings. This condition is called "unstable static stability" or just "unstable." Unstable regions are generally turbulent and associated with daytime heating conditions. Figure 1 (a) displays a near-surface unstable environment, showing warm, less dense air near the surface and the cooler, denser air above. The color coded bubbles show the air parcels from their stating environment, rising to their level of equilibrium.

2. STABLE Static Stability: If the air parcel is cooler than the environment, then the parcel is negatively buoyant and will sink until it reaches equilibrium with its surroundings. This condition is called "stable static stability" or, just "stable." Stable regions are mostly laminar or non-turbulent, and often associated with rural nighttime cooling conditions.

Figure 1 (b) displays the atmospheric stable environment, with layers of cooler, denser air near the surface and warmer, less dense air aloft.
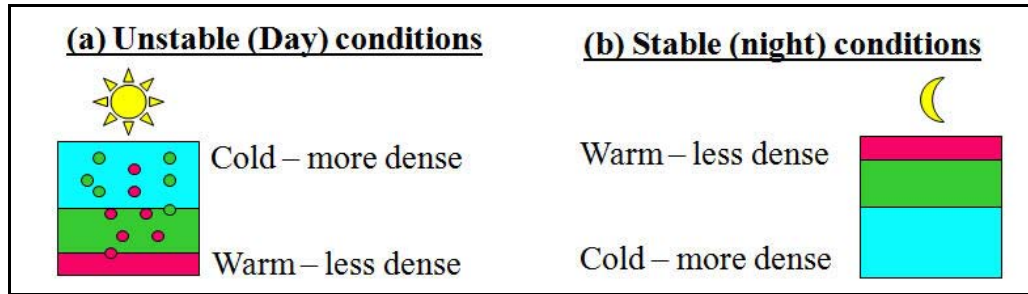
Figure 1. (a) Unstable Atmospheric Conditions are associated with typical daytime conditions. The warm air over the surface bubbles upward until it reaches a state of equilibrium with the ambient atmosphere; (b) Stable atmospheric conditions are associated with night time conditions.

3. NEUTRAL EVENT: The diurnal transition between the unstable and stable scenarios is called a "Neutral Event" or "NE," since conditions are neither unstable nor stable. This NE will be elaborated on later in the text (Stull, 2000).

1.2 Atmospheric Stability and Density Relationships

Cold air is denser than warm air. The Ideal Gas Law presents this relationship mathematically:

$$P = \rho RT , \tag{1}$$

where P is pressure, ρ is density, R is the universal gas constant for dry air, and T is temperature.

Isolating density (ρ), one can see that density is inversely proportional to temperature:

$$\rho = \frac{P}{RT} . \tag{2}$$

Thus, at a constant pressure level, when density increases, temperature decreases, proving the initial statement.

In section 1.1, an air parcel that was warmer (less dense) than its surroundings was labeled "unstable" and if given an initial kick, would rise until equilibrium was reached between the air parcel and its environment. If one were to generate a temperature profile in such an environment, then the lower temperature sample would be warmer (less dense) than the upper sample (more dense). Calculating the temperature difference (ΔT), the value would result in a negative number:

$$\Delta T = T_{upper} - T_{lower} . \tag{3}$$

Applying this concept to the "stable" environment, the air parcel that is colder (more dense) than its surroundings would sink downward to its equilibrium position. The vertical temperature

profile generated would consist of a near surface temperature that was colder (more dense) than the upper temperature. So, ΔT would be positive.

Finally, when the stability is neutral, there is no density variation between the air parcel and the environment. Thus, there would be no temperature gradient and ΔT would be zero or isothermal.

The one qualification that needs to be included with the stability and ΔT relationships, however, is that the atmosphere has a well-known systematic temperature decrease with height throughout the boundary layer (troposphere). The rate that the temperature decreases is called, "the Lapse Rate". When the atmosphere is dry, the standard dry adiabatic lapse rate is -9.8 °C/km. Temperature gradients that cover a large vertical area in the boundary layer (i.e., 100's of meters) need to have the dry adiabatic lapse rate removed from the data before being utilized by models/algorithms. For this study, however, the vertical difference was less than 8 m. The systematic imposition by the lapse rate was less than -0.08 °C/m. In an operational optical propagation environment, this "correction" was not considered significant. Therefore, it was not be included in the analysis. The appendix discusses this correction in more detail.

1.3 Linking Stability, Vertical Temperature Gradients, and Turbulent Parameters

A coherent light travels along an unobstructed path within the Surface Layer. How would you characterize the horizontal path (volume) of air, and its impact on the coherent light?

Using a classical, academic micrometeorology education, the approach for answering this question would probably begin with the use of standard meteorological variables such as, Pressure, Temperature, Relative Humidity, Wind Speed and Direction, and Solar Radiation. Coherent light is strongly impacted by atmospheric stability (density) and turbulence; therefore, the next step would be to use the standard variables to calculate the Richardson Number (a ratio of buoyancy and wind shear) to determine when the atmosphere is turbulent or laminar. The turbulent strength, however, would require expanding the micrometeorology discipline to include atmospheric optical propagation parameters, namely structure functions. Structure functions are difficult to validate, though costly sensors such as scintillometers are available to acquire these measurements. Turning to an operational laser test environment, these measurements can be routinely collected. Ironically, from the operational environment experience, one quickly learns that there are simpler, less costly measurements based on the vertical temperature gradient that correlate with the structure functions that can be used to answer the initial surface layer characterization request. Completing this loop of logic, these near surface, vertical temperature gradients can be used to define the atmospheric static stability along the initial laser beam path. From this atmospheric static stability, the turbulent character of the path, as it pertains to optical propagation, is implied.

In this report, the less costly temperature gradient measurements for characterizing the static stability and implying the near-surface turbulent character of an urban test site were used. For the scientist unfamiliar with the relationships between the above terms and parameters, the

appendix addresses the various mathematical links and offers additional references for the ambitious investigator.

1.4   Atmospheric Optical Propagation

Atmospheric stability has a significant impact on electro-optical (EO) beam propagation. In a vacuum, EO propagation is undistorted in time and space. When the atmosphere is the propagation medium, random irregularities within the atmosphere or, atmospheric optical turbulence (AOT), alter the beam path significantly.

AOT manifests in several forms. For example, when the atmosphere consists of a mixture of hot and cold air pockets, a beam of light will constantly bend toward the colder temperatures (greater densities) and appear to twinkle. This scintillation degrades the image and can even cause it to breakup or blur. Other observable effects are a function of turbulent eddies found within the atmosphere.   When turbulent eddies are larger than the propagating beam diameter, the coherent beam will appear to "wander." When turbulent eddies are smaller than the beam diameter, the beam "spreads." Figure 2 schematically summarizes these three main AOT effects.
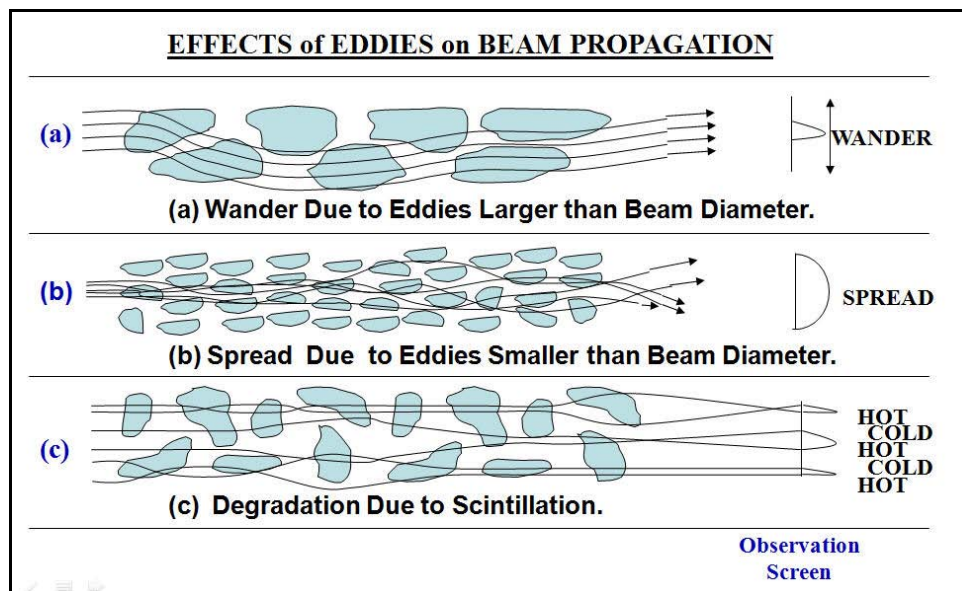
Figure 2. Atmospheric optical turbulence effects on the propagation of a coherent high energy laser.

To minimize the atmospheric impact on a propagating beam, a homogeneous or near-homogeneous atmosphere is required. This condition occurs naturally in a rural environment. It is not a vacuum; however, it does take on the vacuum's attribute of being a medium with a consistent density along the propagation path.   In the rural desert environment, this condition occurs twice a day: once in the morning and once in the evening. NEs near the surface are forecastable, as explained in earlier sections.

1.5 Rural Neutral Events and their Electro-Optical Application

A typical rural, near-surface, stability cycle consists of unstable conditions in the daytime, stable conditions at night and two NEs (around sunrise and sunset) that link the day and night time patterns. The primary attribute of an NE is that the atmosphere is as close to homogeneous in character as the natural environment can produce.

For EO propagation through the atmosphere, these time periods provide the ideal scenarios for investigating EO propagation hardware in an open environment. Put simply, during the NE, the atmospheric effects are reduced to a minimum, allowing the tester to more clearly observe the non-atmospheric EO propagation influences, which is typically, the system hardware. (The optimal nature of the NE presumes that the high energy beam is sufficiently aspirated to eliminate thermal blooming effects.)

The duration of a rural, desert NE can be as short as 1 min or, more than an hour. The length of time is dependent on several factors. Before describing these factors, we need to establish the definition of a "normal" NE.

A "normal sunrise NE" is defined as the transition of nighttime stable conditions to daytime unstable conditions under a horizon-to-horizon, clear sky and in open terrain, such as a desert. The expected duration of this NE would be 1 min. In this "normal" scenario, sunrise begins with unobstructed solar heating of the ground. On the solar equinox, 60 min of solar heating would be needed before the surface layer becomes sufficiently warmed, to create a homogenous environment within the surface layer. The isothermal environment, however, does not stagnate under the unimpaired solar heating. Instead, the ground's continued thermal warming immediately transitions the atmosphere above it into unstable conditions. These unstable conditions will persist throughout the day, until the uninterrupted solar heating wanes on the western horizon.

For a "normal sunset NE," the sky must again be clear from horizon-to-horizon and the terrain un-obscured by shadow-casting figures. This scenario allows the ground to initiate an uninterrupted release of the day's heat prior to the earth's obstruction of the incoming solar rays. The early heat reduction is due to a combination of the incoming solar angle and the atmosphere through which the surface heating is being conveyed. That is, when the sun nears the horizon, the amount of atmosphere through which the sun rays travel increases to about 26 times that of solar noon (McCartney, 1976). At the equinox, the relative timing for when the near-surface atmosphere reaches a homogeneous state is about 40 min prior to sunset. The clear sky allows the radiative cooling to continue without interruption, so that the stable environment commences within a minute of reaching the isothermal NE state. Thus, what we define as a 'normal' sunset NE generally lasts for only 1 min.

In Vaucher and Bustillos (2003a), two additional NE types were observed: Extended and Multiple NE. The "Extended" NEs were associated with overcast, windy days. Interpreting the

sunrise Extended NE scenario reported in the publication, once the homogenous NE environment was reached, a cloud cover obscured the solar heat source, preventing the "normal" quick transition between the night- and day-time stability conditions. Thus, the NE conditions were extended. Once the solar disc reappeared, the surface heating resumed and the transition to unstable conditions occurred. Note: The reappearing of the solar disc was at a higher elevation so that the solar energy traversed fewer atmospheres to reach the ground. This geometry caused the stability transition to be more efficient.

The "Multiple" NE conditions were also associated with cloud cover and can be reasoned similarly to the Extended NE. The only exception would be that the clouds occulting the sun had several breaks in them. The intermittent heating gained through these cloud breaks provided the surface heating several opportunities to start toward an unstable environment. However, due to the inconsistency in the heating, the local neutral environment temporarily dominated. Thus, the stability results appeared to have multiple periods of NE conditions.

Another factor that impacts NE timing is local ground moisture. Based on the Vaucher and Bustillos (2003a) 2001 field study, the local moisture appeared to act as a retardant to the transition process. This sluggishness appeared to favor the current ambient conditions. That is, if neutral conditions were reached, then the NE would be extended. If the scenario was in a night time stable environment, then a "delayed NE" would be observed. These "delayed NEs" or prolonged stable conditions, were not only a function of local ground moisture, but also local shadowing. When comparing the rural and urban stability cycles, the local environment was very important.

1.6 Rural Neutral Events and a Convective Modeling Application

Researching atmospheric optical propagation prompted the current stability cycle investigation. However, there are other applications that utilize the forecasted NE. Atmospheric convective modeling, while well understood, needs to know when to initiate the convection (unstable atmosphere) in their models. Grimsdell and Angevine (2002) focused their research on the afternoon stability transitions in an agricultural environment, citing that the period between the fully developed convection of mid-day and the stable conditions of the nocturnal Boundary Layer was poorly understood.

Other professional disciplines that gain from an improved understanding of the NE period include chemical and pollutant dispersion modeling. The unstable atmosphere tends to disperse airborne substances more quickly than stable or neutral conditions. When the transition to an unstable condition is forecasted to occur it thus becomes important information to the biological or chemical dispersion modeler.

Before rural and urban stability cycles can be compared, each pattern needs to be understood. In the following two sections, the rural and urban stability cycles will be independently defined and discussed.

2.   The Rural Diurnal Stability Cycle

Section 1.5 explained that a typical rural stability cycle consisted of unstable conditions in the daytime, stable conditions at night and two NEs that linked the day and night time extremes. While forecasting the evolution of surface layer stable or unstable environments is beyond the scope of this report, what follows describes the forecasting of two key anchor points in the rural diurnal stability cycle: the sunrise (morning) NE and the sunset (evening) NE.

2.1   Rural Neutral Event Forecast Model

Forecasting the time for an NE in the mid-latitudes begins with the general empirical formulae:

$$\text{Sunrise NE time} = \text{sunrise} + 60 \text{ minutes}; \tag{4}$$

$$\text{Sunset NE time} = \text{sunset} - 40 \text{ minutes}. \tag{5}$$

Vaucher and Endlich (1994) examined a years worth of sunrise/sunset NEs in a rural desert environment and observed a fairly well-behaved annual cycle that enabled them to refine the generic equations. The refined equations were published in a report by Vaucher and Endlich (1995). These NE Forecast Model equations were:

$$\text{Sunrise NE time} = \text{sunrise} + 60 \text{ minutes} + \text{correction}; \tag{6}$$

$$\text{Sunset NE time} = \text{sunset} - 40 \text{ minutes} + \text{correction}, \tag{7}$$

where the correction is:

$$\text{correction (in minutes)} = a_0 + \Sigma_n \left(a_n \cos n\theta + b_n \sin n\theta \right), \text{ where n=0 to 6}, \tag{8}$$

and the coefficients are given in tables 1 and 2.

Table 1. Sunrise NE coefficients.

Sunrise Subscript n	a_n	b_n
0	3.60	0
1	3.83	1.86
2	6.04	7.72
3	0.217	0.358
4	-0.798	0.150
5	0.0714	-0.221
6	0.138	0

Table 2. Sunset NE coefficients.

Sunrise Subscript n	a_n	b_n
0	6.36	0
1	6.48	1.46
2	7.60	8.96
3	0.768	-0.512
4	-0.348	-0.950
5	0.377	-1.61
6	-0.234	0

2.2   NE Forecast Model Validated in Alternate Desert Environment

In 2001, the refined and operational NE Forecast Model was brought to an alternate rural desert site in the southwestern U.S. The success at the alternate site was documented in three technical reports (Vaucher et al., 2003a, 2003b, 2003c).

3.   The Urban Diurnal Stability Cycle.

The urban atmosphere is quite different from the rural environment referenced in sections 1 and 2. In fact, there is quite a diversity of interpretations for the term "urban environment." These interpretations range from large cities to small building complexes. For this research, the "urban environment" was defined as "a small urban building complex." Small building complexes are susceptible to local forcing factors. To help understand these factors, a description of the "small urban building complex" used in this study follows:

> The regional environment for the area studied was the United States southwestern desert. The subject office building was a rectangular, two story building surrounded by similar office buildings on three sides. A four-row parking lot and a four-lane street were located on the fourth side, which climatologically was downwind (leeside) of the subject building. Nearly-level gravel filled the spaces between buildings; however, there was a grassy area between the subject building and the always empty, four-row parking lot.

The urban site referenced was the sampling site for three independent urban field studies conducted by the U.S. Army Research Laboratory (ARL). The field studies were called, *WSMR[1] 2003 Urban Study* (*W03US*), *WSMR 2005 Urban Study* (*W05US*) and *WSMR 2007 Urban Study* (*W07US*). All three field studies used the same single subject building and acquired data over the March/April time period. The March (vernal equinox) time period was selected to minimize the systematic seasonal influences (a balanced solar heating/cooling cycle) and to utilize the New Mexico "windy season." Each successive field experiment increased the temporal and spatial data sampling resolution. Data from these field studies will be used to demonstrate the three

---

[1] WSMR is White Sands Missile Range, NM.

urban stability cycles described in section 3.1. The urban site was selected based on its about 35 km proximity to the original site used to develop the (rural) NE Forecasting Model described in section 2.

3.1 Three Urban Diurnal Stability Cycles.

The first concept that comes to mind when discussing urban stability is the Urban Heat Island (UHI) effect. UHI is generally used to describe a large city where the core is warmer than the outer edges. When isothermal lines are drawn over the large city they appear to form concentric circles, similar in appearances to an island topography map; thus, the term "UHI" is used. This concept is not only applicable to a large city, but can also be applied to a single, occupied office building. The horizontal temperature gradient framing the building might be smaller, depending on the local scenario; however, with the building being warmer than the surrounding area, a mini-UHI is still possible. For this reason, urban modelers tend to integrate unstable or unstable/neutral stability conditions into their models. However, these are not the only choices.

Three diurnal urban stability cycles were observed in the ARL urban field studies. These were:

- 24 hours of unstable conditions.

- 24 hours of unstable and neutral conditions.

- 24 hours of unstable, neutral and stable conditions.

As previously mentioned, the first two urban diurnal patterns are generally utilized by urban modelers, when inputting stability conditions into their models. For small building complexes, however, all three patterns are valid. Each urban cycle will be described in the following. The general atmospheric scenario underlying the cycles was a clear sky.

3.1.1 Always Unstable (1-State Stability) Cycle

The persistence of unstable conditions was primarily due to solar and anthropological influences on the urban environment. During the daytime, the incoming solar radiation provided the primary heat resource. Local humanity also contributed to the heat, through various activities such as artificially heating the buildings and vehicular traffic. Since the Study scenario prohibited automotive traffic near the subject building during the observing period, the potential automotive heat resources were minimized. Dark colors of the pavements and building features absorbed and re-radiated more energy over time than reflective colors. The absence of shade (urban desert environment) also promoted a continually unstable environment through the ground heating.

At night, radiative cooling was a dominant process. However, due to the amount of energy absorbed throughout the day, the time needed to achieve a net radiation loss took the entire sunless period. Add to this the anthropological factor of heating the building at night, as well as low winds to transport the heat away from the building site, and a 24-h period of unstable

9

conditions resulted. Using ΔT to quantify stability, figure 3 displays a clear example of an "always unstable" cycle that occurred around a small urban building complex on 2003 March 28 [JD# 87] (blue time series).[2] The data plotted were sampled from the south side of the subject building, in a ventilated and solar-wise exposed urban canyon. Winds for 2003 March 28 were generally out of the southeast, between 0 and 8 m/s. This day's solar radiation showed a mid-day maximum of 1275 W/m^2 (a *W03US* solar radiation maximum).
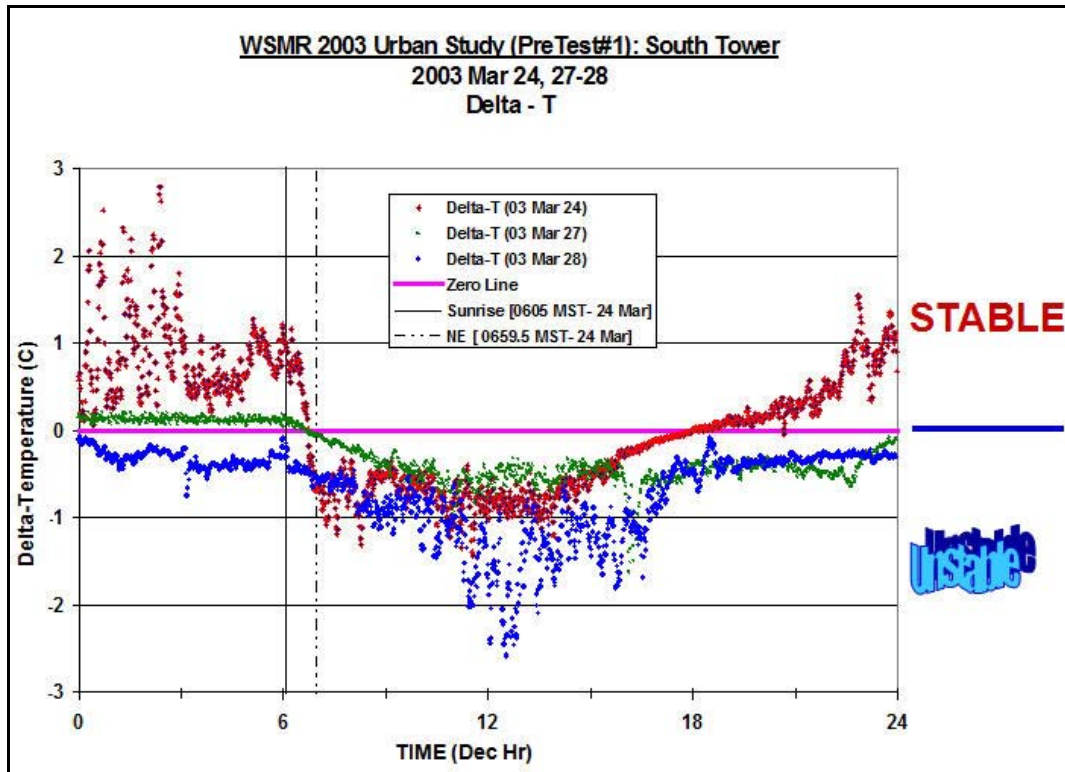
Figure 3. *W03US* field study analysis reported 24-h cycles which were composed of unstable conditions only (blue line-2003 March 28), unstable and neutral conditions (green line-2003 March 27) , and also, unstable, neutral and stable (red line-2003 March 24) atmospheric conditions.

The day prior to this "always unstable" cycle was a mixed "unstable and neutral" diurnal cycle. Section 3.1.2 will describe this case.

3.1.2 Unstable and Neutral (2-State Stability) Cycle

When the night time radiative cooling rates increased, a period of neutral or near neutral conditions was possible. On 2003 March 27 [JD# 86], the *W03US* data plotted in figure 3 (green time series) shows a neutral and near-neutral atmospheric condition from midnight through sunrise (0605 LT).[3] The hour following sunrise shows an NE transition. In this case, the change was from a near-neutral state into an unstable condition. The subsequent atmospheric conditions

---

[2] JD is the Julian Date.

[3] LT is local time (mountain time).

persistently remained in the unstable state throughout the daylight hours and into the night. Near midnight, the stability state approached a neutral environment, but did not actually transition. Instead it returned to unstable conditions throughout the next day (see section 3.1.1). Wind for 2003 March 27 was primarily westerly, ranging from 0 to 17.8 m/s (a field study maximum). Solar radiation maximum for this date was 1078 W/m^2.

3.1.3 Unstable, Neutral, and Stable (3-State Stability) Cycle

The 24-h pattern of "stable (night), neutral (near sunrise), unstable (day), neutral (near sunset) and stable (night)" would normally characterize a rural atmospheric cycle. However, on 2003 March 24 [JD# 83], this tri-state stability pattern was clearly evident (see figure 3 red/brown time series). Stable samples occurred from midnight past sunrise (0605 LT). Shortly before the calculated NE (rural NE Forecast Model), the atmosphere recorded a very quick transition from stable to unstable. The hasty stability transition settled into consistently unstable conditions throughout the day. However, once the sunset hours started to approach, a gradual transition back into a stable state occurred. The well-behaved curve mapping this transition and subsequent increasing trend into the stable environment climaxed around the midnight time period. The association of midnight and stable urban environments was very strong throughout all three field studies. Section 3.2 elaborates this observation. The relatively large, positive ΔT magnitudes reported in this south tower example were also observed on all sides of the building during the *W03US* field study. Wind on 2003 March 24 was primarily northwesterly, ranging from 0 to 12.6 m/s. Solar radiation maximum for this date was 975 W/m^2.

3.2 Urban Stable Attributes.

Observing a stable environment in all three ARL single-building urban field studies was unexpected. Therefore, an inter-study comparison was conducted to better understand this unusual state. In each of the three field exercises, 10-m and 12-m towers were positioned on each side of the north-south aligned, two-story subject building. A tripod (6 m tall) was mounted on the roof for the latter two experiments. However, only the third experiment included roof stability sensors. Figure 4 shows the layout schematically. Prevailing winds for the site were from the southwest, as shown by wind vectors and its correlated 3-Dimensional Wind Field (3DWF) Model run.
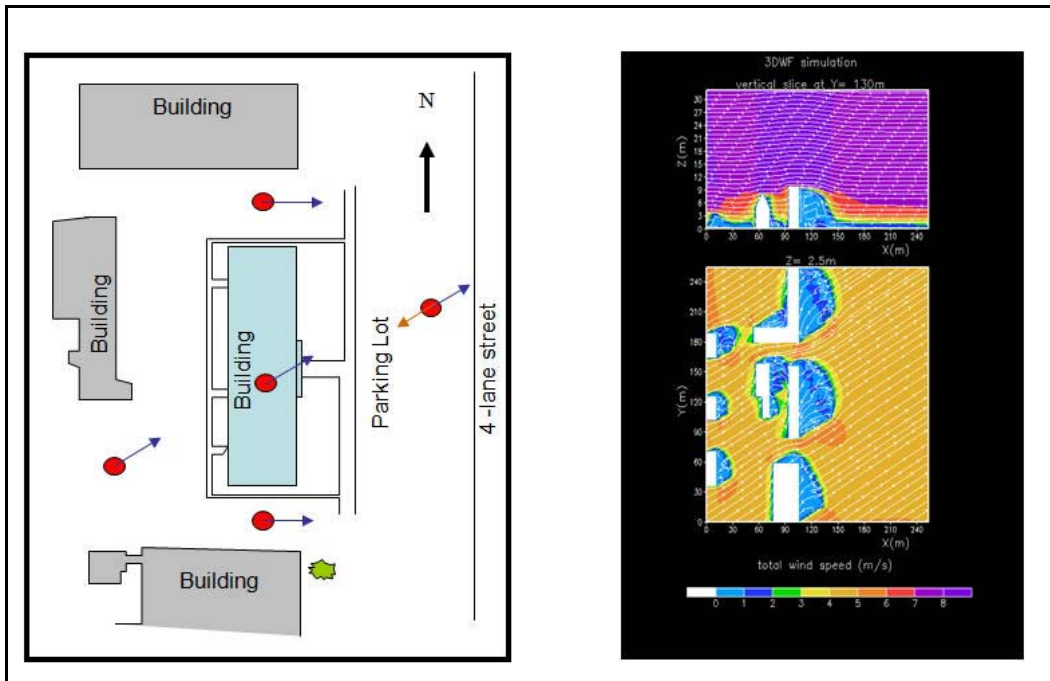
Figure 4. *W03US, W05US* and *W07US* used 10 m and 12 m towers strategically placed in each compass quadrant of the subject building. The latter two field studies also included a roof tripod. The arrows on the schematic show a sample of coincident wind directions. The image to the right is a 3DWF model run based on meteorological data taken from the field study. The leeside cavity flows (flow reversals) were observed both by the measurements and the model (Cionco et al., 2006).

Using the ΔT method for deciphering stability, the following results were observed (sections 3.2.1 and 3.2.2).

3.2.1 Temporal distribution of stable conditions around an urban building.

First, the temporal distribution of stable conditions was analyzed by dividing the 24-h clock into quadrants (see figure 5). Translating each field study into a percentage of total stable minutes (see table 3), the most frequent occurrence for stable conditions occurred between 2100 and 0259 LT. A later analysis subjectively refined this interval to 0000–0259 LT. The second most frequent occurrence was from 0300 to 0859 LT. The temporal distribution results across the three field studies was one of the most consistent attributes observed in the inter-study comparison.

Consecutive minutes of a stable condition were grouped together in what was called "a case." Figure 6 shows a plot of the cases observed during *W07US*. Each color represented cases from a different tower. The average stable case duration, across all three field studies, was 6–8 min. Extreme case lengths were observed from each meteorological tower. Using all three field studies and organizing the results by building side (tower), the extreme cases ranged from 14–312 consecutive minutes. Note that 312 min is more than 5 h! These extreme cases favored

light wind environments. Figure 7 shows the "extreme cases" results with respect to the subject building.
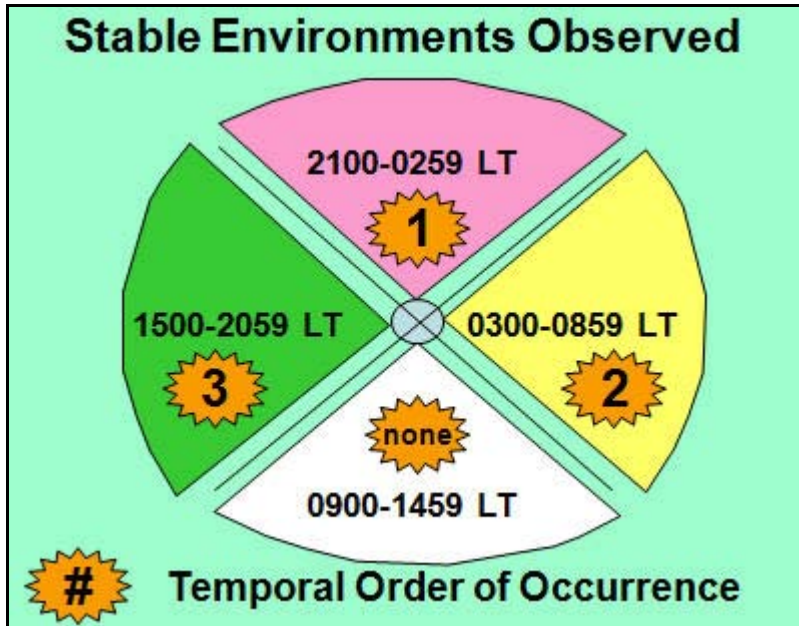
Figure 5. The stable environment temporal distribution was tallied by dividing the 24-h clock into quadrants. The most frequent stable environment occurred from 2100 to 0259 LT. A healthy second was from 0300 to 0859 LT.

Table 3. Stable environment observations were temporally analyzed by dividing the 24-h clock into quadrants and normalizing the totals by total minutes observed. The most frequent stable environment occurred from 2100 to 0259 LT. A healthy second was from 0300 to 0859 LT.

Field Study	Sunrise 0300–0859 LT	Daytime 0900–1459 LT	Sunset 1500–2059 LT	Night Time 2100–0259 LT	Total (%)
W03US	44	0	0	56	100
W05US	44	0	6	50	100
W07US	28	0	6	66	100
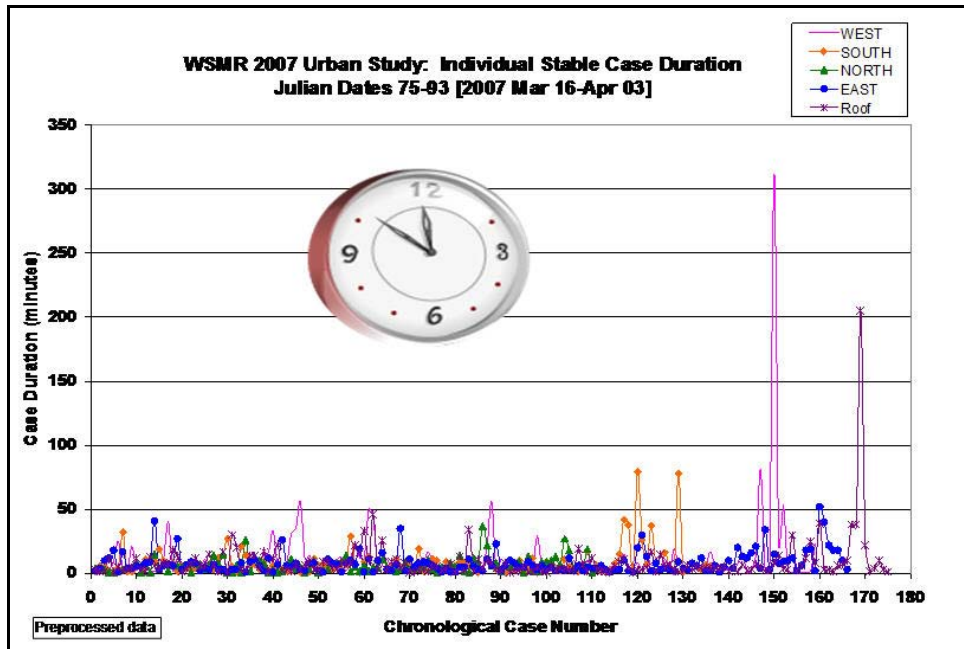
Figure 6. Defining a "case" as a period of stable conditions over consecutive minutes, the follow results were gleaned from *W07US*. The average case length for all three field studies was between 6 and 8 min in length.
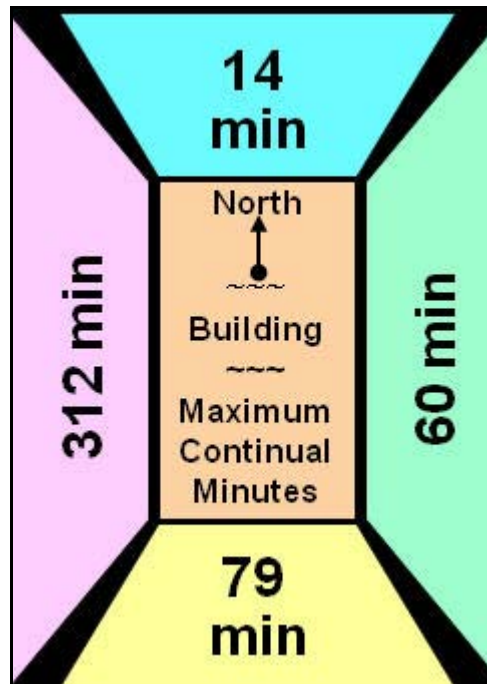
Figure 7. Extreme case lengths were observed in each field study. The diagram shows the subject building in the center, with the maximum continual minutes observed labeled by building quadrant. Extreme stable case durations favored the light wind environments.

14

3.2.2 Spatial distribution of stable conditions around an urban building.

Spatially-across the field study layout, stable environments were observed on all sides of the subject building. Figures 8a and 8b show an example of all four building sides and the roof tripod coincidently reporting stable conditions within a 24-h time period. Figure 8a shows the total number of stable minutes as a function of the *W07US* field study date. Figure 8b shows the stability conditions for a single day (2007 March 20) as a function of time and location (tower) around the subject building.
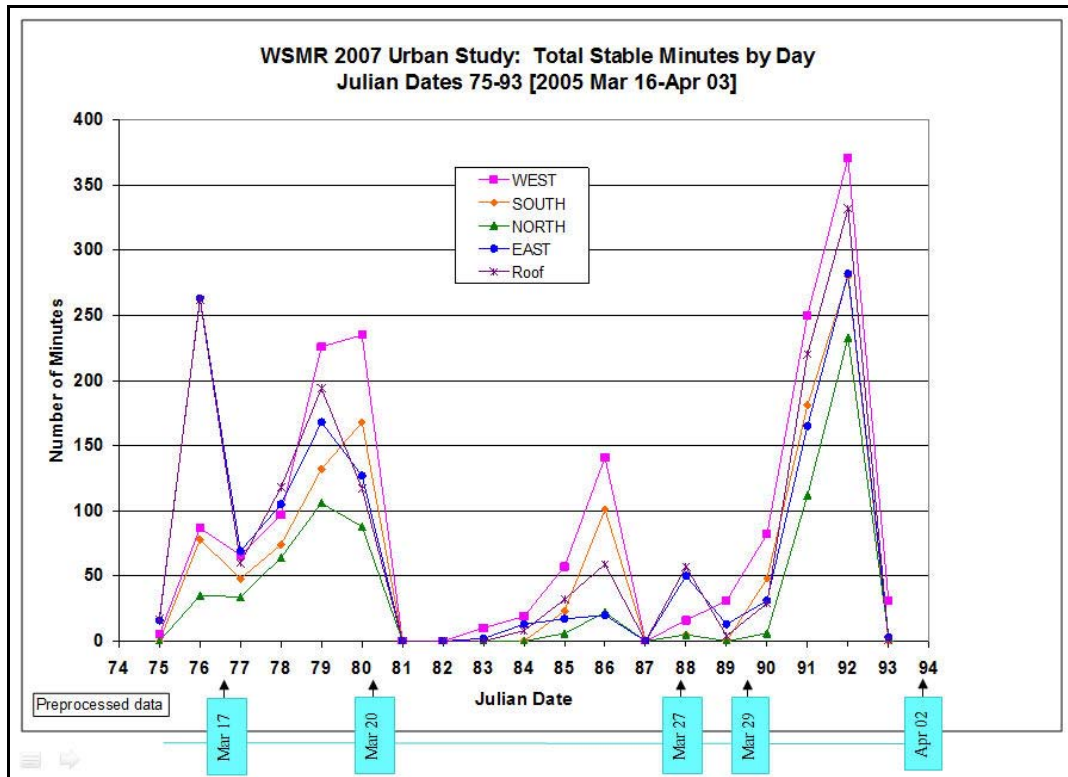
Figure 8a. *W07US* field study reported stable conditions on all four sides and the roof of the subject building. This plot shows the total number of stable minutes records per day.

15
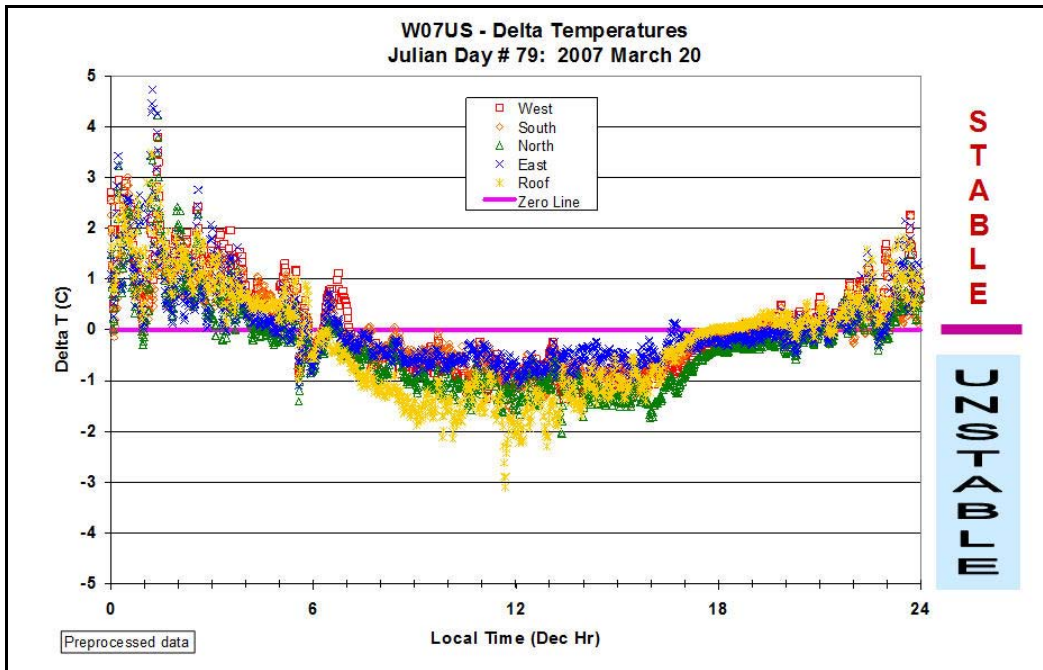
Figure 8b. On 2007 March 20, the *W07US* reported stable conditions on all four sides and the roof of the subject building. This plot shows stability as a function of time and location around the subject building.

During windy conditions, however, the building leeside was favored for a stable environment. The open leeside environment (also, a building wake area) suggested an increased potential for radiative cooling with respect to the other "enclosed" building sides.

During light wind conditions, the building windward was favored for stable conditions. Heat from the radiating building lacked the airflow necessary to send the heat away from the building. Therefore, all sides, but the windward, integrated the added heat into the vertical volume of air next to the building and consequently reported less stable conditions than the non-building-influenced windward (Fetch) side.

The roof with an elevated heating vent, in light wind conditions, generated the second most frequent location for stable environments around the subject building. When the *W07US* field study layout was designed, the regional climatology called for sustained, southwesterly windy conditions over most of the 24-h period. Under these conditions, the roof tripod position was placed well outside of the vented heat flow path. Unfortunately, when the field study acquired data, the climatologically strong southwesterly winds did not always occur. Instead, there were long periods of light winds. Subsequently, the venting heat loitered over the building. Eventually, the pocket of heated air reached the upper temperature sensor of the roof tripod, causing a classic stable environment of warmer conditions aloft and cooler conditions near the roof surface. Figure 9 shows both the expected and the sampled roof data acquisition scenarios.
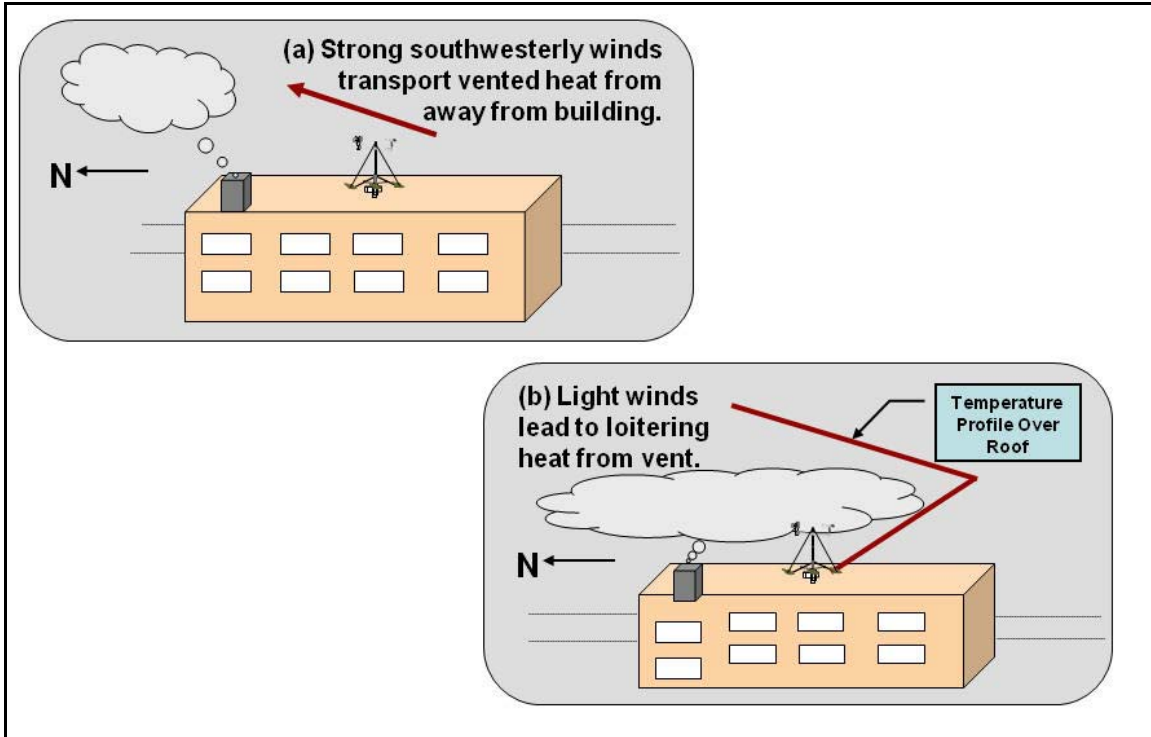
Figure 9. The roof with an elevated heating vent generated a stable environment. (a) The anticipated roof data acquisition scenario; (b) the sampled data acquisition scenario.

4. Comparing Rural and Urban Diurnal Stability Cycles

The purpose for comparing rural and urban diurnal stability cycles was to investigate the possibility of creating an urban equivalent to the (rural) NE Forecast Model. In this context, the comparison begins.

4.1 Comparing Rural and Urban Neutral Event Patterns.

The rural stability cycle model described in section 2 centered on two key anchor points, the sunrise and sunset NEs. These events represented a clear passage from stable to unstable conditions, and visa versa. To construct an equivalent urban stability model requires first identifying repeatable urban NEs that represent a transitory state, and then building forecast algorithms for these "anchor points."

Table 4 summarizes the typical rural and three observed urban stability cycles. Two of the three urban stability cycles reported neutral atmospheric conditions: the Two-State (Unstable-Neutral) and the Three-State (Unstable-Neutral-Stable) cycles. In the Unstable-Neutral cycle example (refer to figure 3) the "sunrise" transition occurred over the same time period as the "sunrise" transition of the Unstable-Neutral-Stable cycle. There was no evening transition. However,

around midnight the conditions neared neutral conditions, again. The important observation is that in an urban setting, the function of a neutral atmosphere is not always for a stability transition. Establishing the criteria for this alternate function was considered important, yet secondary in the modeling effort. Therefore, the task was put on hold until the foundational urban factors were better defined and understood.

Table 4. Comparison of rural and urban diurnal stability cycles.

Local Time	Rural Stability Status	Urban One-State	Urban Two-State	Urban Three-State
2100-0259	Stable	Unstable	NE-Extended	Stable
0300-0859	NE-Sunrise	Unstable	NE-Sunrise	NE-Sunrise
0900-1459	Unstable	Unstable	Unstable	Unstable
1500-2059	NE-Sunset	Unstable	Unstable	NE-Sunset

Turning to the Urban "Three-State" stability cycle: From a gross picture perspective, there did not seem to be any difference in the rural and urban-three state stability cycles. That is, until the urban data were more closely examined. Using the 2007 March 20 Case [JD# 79] (figure 8a), observe the multiple time series as they progress from midnight to sunrise (about 0600 LT). The north tower leans toward the neutral and unstable conditions in advance of all the other sides, even preceding the eastern (sunrise side) tower. The north side data were acquired in an urban canyon. The warmth from the second building may have influenced the multiple early dips into the neutral and unstable region of the stability plot. Coupling this local influence with the sun rising, the sudden surge of unstable conditions reported by the north tower becomes more understandable.

In contrast, using this same midnight to sunrise period, the west side data were more sluggish in making the transition. Shadows, cast by manmade structures, during the sunrise time period may have had an influence on the pre-0600 LT west side data. After sunrise (about 0600 LT), both the west and east towers report a return to stable conditions. The coincident roof and the north towers return to neutral stability conditions, but not to the stable environment. These observations imply a systematic influence—perhaps the presence of thin clouds on the eastern horizon. Unfortunately, after examining the solar radiation time series for each tower, only the west and east data show any discontinuity in the curve for the post-sunrise time period. If cloud occultation was the cause, the resource could have been very thin cirrus. From personal observations, a solar radiometer sometimes has difficulty sensing very thin cirrus clouds. Revising the cause and effects explanation, perhaps thin cirrus initiated the shift back to neutral conditions, but the roof and north towers had sufficient local forcing (heat from a neighboring building or the warmed roof top radiating what little heat it just received during sunrise) to only shift into a neutral condition. The west and east towers had their versions of local forcing, however, the manmade building for the west tower and natural foliage (tree/plant) on the east side was significant enough to affect both the solar radiometer measurements and a shift back into a stable condition.

18

Shifting to the 2007 March 20 Case sunset NE transition, the stability pattern is far less abrupt than the sunrise NE transition. The author has seen these contrasting sunrise/sunset patterns in the 2001 rural data; therefore, defining the cause for this contrast would be a function of the distant horizons. The eastern horizon (sunrise) for the rural and urban sites was the same, a flat mesa-type terrain. The western horizon (sunset) was a jagged mountain range for both locations.

During the sunset NE transition, the roof data arrived at the neutral environment ahead of the other building sides. The north side was the last to make the NE transition. Again, the sluggish transition of the north side may be largely a function of the close proximity and influence of the second building. The eastern data showed an isolated early neutral condition, but then rejoins the gradual transition of the rest of the building-sides right afterwards. The early neutral condition may be partly a function of building shadows. The eastern tower would also have been warmed by the radiating paved parking lot underneath, which may explain the temporary nature of the neutral condition.

When an oscillating rural stability time series occurred between 2000 and 0500 LT, the consensus between colleagues was that this pattern was a signature of gravity wave activity coming off the local mountains and drainage flow cascading down the valley. Seeing a very similar fluctuating pattern in the 2007 March 20 urban data, the initial thought was to suggest that mountain induced gravity waves and drainage flow may be influencing the data. However, due to the complexity of the urban site, the author would tend more toward citing more local influences (natural and anthropological) as being the cause.

4.2   The Urban Neutral Event Forecast Model.

The rural NE Forecast Model was constructed around three foundational influences: the solar angle (time of day) adapted for the season, shadowing (i.e., cloud cover) and ground moisture. After analyzing ARL's three urban field studies, the three principle influences in the urban NE Forecast Model were solar angle (time of day) adjusted for season, shadowing and the greatest local anthropological influence.

The urban "shadowing" included the systematic influence of cloud cover, as well as, various site specific physical structures. As an example of urban physical structures these would include buildings, trees, solid fences, etc. Note: The rural model also included the site-specific structure shadowing, but only as a secondary concern. This decision was based on the flat, desert location in which the original rural model was constructed.

The "greatest local anthropological" influence was site specific. Some examples of these items include radiating or exhausted building heat from the subject and/or neighboring buildings.

The ground moisture was not included in the foundational list for the urban NE forecast model due to the very efficient water management (drains) found in and around public areas. For areas not in the desert, this choice may need to be re-evaluated.

5. Summary

Atmospheric stability cycles impact where we live, grow our food, and how we conduct our business. Examples of stability applications include the transport and dispersion of air pollutants or hazardous chemicals, convective cloud development, which can lead to beneficial rain or to severe storms, and atmospheric optical propagation such as high energy laser transmissions through the open air.

This report documents the urban diurnal stability cycle research, an outgrowth of the ongoing Urban Stability research begun with the *W03US* field project. The long term goal for this investigation is to develop an empirical NE Forecast Model for the urban environment. This quest stems from the success of an NE Forecast Model that was created for an operational high energy laser test facility located in a rural desert environment. NEs represent periods during which the atmosphere had a minimal impact on the laser operation; thus, they have a significant impact on the site mission.

There are at least two methods for understanding atmospheric stability: the classical micro-meteorological approach and the EO propagation applications approach. The classical micro-meteorological approach examines stability through vertical temperature gradients (lapse rates) and micro-meteorological turbulence parameters. The EO propagation applications approach examines stability through atmospheric density variations along a path and atmospheric optical turbulence parameters. The tools used in this urban diurnal stability cycle research utilized both perspectives.

Three urban field studies were conducted by ARL around a single, two-story urban building in a small building complex in southern New Mexico. These studies investigated both the urban stability and wind flow patterns. Based on this dataset, three general urban stability patterns were identified: the Always Unstable (1-state stability) cycle, the Unstable and Neutral (2-state stability) cycle and the Unstable, Neutral and Stable (3-state stability) cycle. Examples of each were presented in this report.

Stable atmospheric conditions are not normally associated with an urban environment. Therefore, a closer look into the character of the stable state was pursued. Drawing from the three urban field studies, temporal and spatial attributes for this unexpected urban stable state were identified as the following:

- The most populated time period for stable conditions occurred between 2100 and 0259 LT.

- The second most frequently stable period was from 0300 to 0859 LT.

- During windy conditions, the building leeside was favored for stable conditions.

- During light wind conditions, the building windward (Fetch) side was favored for stable conditions.

- The average duration of consecutive minutes for stable conditions was 6–8 min.

- The extreme durations for consecutive stable minutes, as defined by the individual tower data, ranged from 14 to 312 min.

- Extreme stable case durations favored the light wind environments.

- The roof with an elevated heating vent generated a stable environment.

With the stable state better understood, the single rural and three urban stability cycles were re-examined. Two urban patterns contained neutral conditions. The Neutral condition was the key element in creating the rural NE Forecast Model. Neutral events were defined as those periods in which the atmosphere transitions between stable and unstable (and visa versa) conditions. The time-extended neutral environment of the two-state urban cycle was deemed important, but a secondary effect, next to the transitory NE function of the three-state urban cycle. Focusing on this three-state cycle with its transitory NEs, the gross diurnal pattern appeared to be nearly identical to the rural stability cycle. Examining the urban cycle as a function of which side of the building was being studied, there were several distinguishing attributes.

The *W07US*-2007 March 20 Case was used to demonstrate the morning and evening NE character for each side of the building. The abrupt nature of the morning NE and the gradual transition in the evening NEs imitated the rural time series data collected within 30 miles of the site. Therefore, this pattern was identified as being a function of the common (rural and urban) eastern and western horizons. The temporal order in which the building sides reported an NE transition seemed to be a function several factors. The four identified were "solar angle" adjusted for season, "systematic shadowing," "site-specific shadowing," and the "greatest local anthropological influence." The top two influences for the urban NE Forecast Model were also the top two factors for the rural NE Forecast Model. That is, the solar angle (sunrise/sunset time of day) adjusted for season and, the systematic shadowing, or cloud effects. The "site specific" shadowing was due to structural resources such as buildings, trees, fences, etc. This influence was a factor for the rural model too; however, since the field tests from which the model was created were conducted over a relatively-flat, open, desert terrain, the effects were not significant. The "greatest local anthropological influence" consisted of items such as the subject building's or neighboring building's heat. This heat could take the form of infrared radiation or vented exhaust. Ground moisture was a foundational influence for the rural NE Model. However, due to the efficient water management in urban areas, this contribution was not considered a significant factor.

This report concludes that, based on the above study, the Rural and Urban NE Models could be summarized as follows:

RURAL Neutral Event Forecast Model

NE = Solar Angle + Systematic Shadowing + Ground Moisture

URBAN Neutral Event Forecast Model

NE = Solar Angle + Systematic Shadowing + Site-specific Shadowing
        + the Greatest Local Anthropological Influence

In future research studies, the qualitative urban stability cycle equation(s) will be converted into mathematical representations and tested against the existing datasets. Due to the complexity of the urban environment, these equations will likely consist of both empirical observations and basic physical principles.

6. References

Cionco, R.; Vaucher, G.; D'Arcy, S.; Bustillos, M. Near-building turbulent intensities, fluxes, and vortices. *14th Joint Conference on the Applications of Air Pollution Meteorology with the Air and Waste Management Assoc., 6th Symposium on the urban environment*, American Meteorological Society, February, 2006. http://ams.confex.com/ams/Annual2006/techprogram/paper_101456.htm (accessed September 1, 2009).

Clifford, S.F., The Classical theory of Wave Propagation in a Turbulent Medium. Topics in Applied Physics. *Laser Beam Propagation in the Atmosphere,* v. 25, Springer-Verlag, Germany, 1978.

Glickman, T. S. *Glossary of Meteorology;* 2nd ed.; AMS: Boston, MA, 2000.

Grimsdell, A. W.; Angevine, W. M. Observations of the Afternoon Transition of the Convective Boundary Layer. *Journal of Applied Meteorology* **2002** (January), 3–11.

Hecht, E.; Zajac, A. *Optics*, Addison-Wesley Publishing Company: CA, 1974.

Jenkins, M. Wildland Fire Management and Planning (Utah State University Class WILD4520, Spring 2004), Unit 7: Atmospheric Stability and Instability. http://ocw.usu.edu/Forest__Range__and_Wildlife_Sciences/Wildland_Fire_Management_and_Planning/Unit_7__Atmospheric_Stability_and_Instability_1.html (accessed February 2, 2009).

McCartney, E. J. *Optics of the Atmosphere, Scattering by Molecules and Particles;* Wiley-Interscience, Wiley: New York, 1976; pp102–113.

Snell's Law, http://en.wikipedia.org/wiki/Snell's_law, (accessed Feb 13, 2009).

Stull, R. *Meteorology for Scientists and Engineers*; 2nd ed.; Brooks/Cole Thompson Learning: Pacific Grove, CA, 2000.

Stull, R. *Introduction to Boundary Layer Meteorology*; Kluwer Academic Publishers, 1988.

Tatarski, V. I., *Wave Propagation in a Turbulent Medium.* Dover Publications, Inc.: New York, NY, 1961.

Vaucher, G.-T.; Bustillos, M. *Surface Layer Stability Transition Research, Maximum Time Delay from Sunrise/Non-Ideal Conditions: 2001 June Case Study*; ARL-TR-2823; U.S. Army Research Laboratory: White Sands Missile Range, NM, 2003a.

Vaucher, G.-T.; Bustillos, M. *Surface Layer Stability Transition Research, Minimum Neutral Event-to-Sunrise Time Interval: 2001 September Case Study*; ARL-TR-2827; U.S. Army Research Laboratory: White Sands Missile Range, NM, 2003b.

Vaucher, G.-T.; Bustillos, M.; Gutierrez, A. *Surface Layer Stability Transition Research, Minimum Time Delay from Sunrise: 2001 March Case Study*; ARL-TR-2798, U.S. Army Research Laboratory: White Sands Missile Range, NM, 2003c.

Vaucher, G.-T.; Endlich, R. Forecasting Atmospheric Optical Turbulence Neutral Events-Part II. *Proceedings of the 1995 Battlefield Atmospheric Conference*, U.S. Army Research Laboratory, White Sands Missile Range, NM, December 5–7, 1995.

Vaucher, G.-T.; Endlich, R. Forecasting/Modeling the Atmospheric Optical Turbulence Neutral Events over a Desert Environment. *Proceedings of the 1994 Battlefield Atmospheric Conference*, U.S. Army Research Laboratory, White Sands Missile Range, NM, November 29–December 1, 1994.

Appendix. Linking Stability, Vertical Temperature Gradients, and Turbulent Parameters Mathematically

In section 1.3, a logical progression linking micrometeorological parameters and parameters used for atmospheric optical propagation was presented. The application drawing these disciplines together was stated to be the following:

> "A coherent light travels along an unobstructed path within the Surface Layer. How would you characterize the horizontal path (volume) of air, and its impact on the coherent light?"

As a review, here is the logical progression presented in section 1.3:

> "Using a classical, academic micrometeorology education, the approach for answering this question would probably begin with the use of standard meteorological variables such as, Pressure, Temperature, Relative Humidity, Wind Speed and Direction, and Solar Radiation. Coherent light is strongly impacted by atmospheric stability (density) and turbulence; therefore, the next step would be to use the standard variables to calculate the Richardson Number (a ratio of buoyancy and wind shear) to determine when the atmosphere is turbulent or laminar. The turbulent strength, however, would require expanding the micrometeorology discipline to include atmospheric optical propagation parameters, namely structure functions. Structure functions are difficult to validate, though costly sensors such as scintillometers are available to acquire these measurements. Turning to an operational laser test environment, these measurements can be routinely collected. Ironically, from the operational environment experience, one quickly learns that there are simpler, less costly measurements based on the vertical temperature gradient that correlate with the structure functions that can be used to answer the initial surface layer characterization request. Completing this loop of logic, these near surface, vertical temperature gradients can be used to define the atmospheric static stability along the initial laser beam path. From this atmospheric static stability, the turbulent character of the path, as it pertains to optical propagation, is implied. "

In the next few sections, the above variables and parameters will be described as a function of the various mathematical links between them.

A-1. Step 1–Data Resources

Characterizing a volume of air is accomplished by first acquiring data for the standard meteorological variables: pressure, temperature, relative humidity, wind speed, wind direction and solar radiation. In this example, point samples of each variable are presumed to be collected at a representative location within the given volume and at the following elevations:

10 m AGL – Wind Speed/Direction, Temperature

2.5 m AGL – Wind Speed/Direction, Temperature, Relative Humidity

2 m AGL – Solar Radiation

1 m AGL – Pressure

A-2. Step 2–Temperature Conversions

An academically-trained meteorologist would begin the air volume characterization by first converting the ambient temperatures into Potential Temperatures (θ). The function of θ is to remove the temperature variations caused by changes in pressure altitude of an air parcel (Stull, 1988). This systematic change for a dry atmosphere, can be quantified by the atmospheric lapse rate of -9.8 °C/km. There are two common equations used to convert temperatures into potential temperatures:

$$\theta = T * (P_o/P)^{R_d/C_p} , \tag{A1}$$

where T = ambient temperature,

P_o = reference pressure (usually 100 kPa or 1000 mb),

P = ambient pressure,

R_d = gas constant for dry air,

C_p = specific heat at constant pressure for dry air.

Equation (A1) brings the given temperature dry adiabatically to a reference pressure, which is commonly defined as 100 kPa or 1000 mb. For boundary layer work, however, the surface pressure can be used instead (Stull, 1988).

$$\theta(z) = T(z) + \Gamma_d * z , \tag{A2}$$

where $T(z)$ = ambient temperature (in C or K) at a given height above ground,

Γ_d = the negative of the dry adiabatic lapse rate (9.8 °C/km),

z = the height above the reference level (100 kPa or surface level).

Equation (A2) is a first order approximation of potential temperature. This equation is often used when height is the vertical coordinate.

Since the cumulative *W07US* dataset was sampled within 20 m of the ground. Equation (A2) was selected for this analysis. The net effect was to inflate the temperatures taken at the 10 m levels by +0.098 °C, and the 2.5 m temperatures by +0.0245 °C.

Since the final analysis used a temperature difference, the net change between using a raw temperature difference and a θ difference was 0.0735 °C. This adjustment, while used to demonstrate the analysis methods, was not considered significant for the final data applications.

A-3. Step 3–Richardson Number Calculations

The next step for characterizing the air volume was defining when the *W07US* atmospheric is turbulent or laminar. The empirically derived Richardson Number does this task. The Richardson Number can be calculated in several ways. Two formulas will be explained here.

The flux Richardson Number is a ratio between buoyancy and wind shear of the Turbulence Kinetic Energy equation. This ratio is approximately equal to what's called the Gradient or Bulk Richardson numbers.

A-3.1 Gradient Richardson Number

The "Gradient Richardson Number" or "Ri" is:

$$Ri = \frac{(g/\bar{\theta}_v)(\delta\bar{\theta}_v/\delta z)}{[(\delta\bar{U}/\delta z)^2 + (\delta\bar{V}/\delta z)^2]} \quad , \tag{A3}$$

where g = gravity,

θ_v = virtual θ,

$\bar{U}$ = the u wind component,

$\bar{V}$ = the v wind component,

z = height.

We will presume the atmosphere is dry (desert), so that θ can be used in place of the θ_v. For more information see Stull (1988).

From empirical studies, the following interpretation standards have been accepted for Ri results:

- When $Ri < R_c$, then the laminar atmosphere flow becomes turbulent or dynamically unstable. R_c is the critical Richardson Number of 0.25.

- When $Ri > R_T$, then the turbulent flow becomes laminar. $R_T = 1$.

Note: $R_T > R_c$ is due to hysteresis. That is, Ri of non-turbulent flow must be lowered to R_c for turbulence to set in. But once conditions are turbulent, the turbulence will continue until Ri is raised above R_T.

A-3.2 Bulk Richardson Number

A second Richardson equation is the Bulk Richardson Number or R_B. When local gradients are not known than an approximate gradient, taken from a series of discrete height intervals, is used. This approximation allows the user to convert the partial differentials into finite differences. That is, from $\delta u/\delta z$ to $\Delta u/\Delta z$. The R_B formula is:

$$R_B = \frac{g * \Delta \bar{\theta}_v * \Delta z}{\bar{\theta}_v \ [(\Delta \bar{U})^2 + (\Delta \bar{V})^2]} \ , \tag{A4}$$

where $\Delta \bar{U} = \bar{U}(z_{top}) - \bar{U}(z_{bottom})$.

Interpreting the R_B result follows the same strategy as the Gradient Richardson Number (Stull, 1988).

A-4 Step 4 - Operational Atmospheric Optical Propagation Parameters

The Richardson Number is an empirical formula indicating the presence of turbulence or laminar conditions. Ri does not quantify the turbulence. To quantifying the turbulence, a statistical parameter associated with atmospheric optical turbulence (AOT) can be used. Though the foundational AOT theory is complex, there are standard operational procedures which link the quantified AOT with the vertical temperature gradient. From section 1, we know that the temperature gradient and static stability are correlated. Therefore, we will present an overview of the foundational theory for quantifying AOT, followed by an alternate, more linear explanation linking index of refraction with temperature. Note: A demonstration showing the link between quantitative AOT measurements and ΔT concludes this appendix.

There has been a significant amount of research done in AOT. What is covered here will include only the most basic concepts and their associated mathematical representations. See Tatarski (1961) and Clifford (1978) for additional information.

A-4.1 Quantifying Atmospheric Optical Turbulence

Light propagates through the atmosphere in the form of a wavefront, or "a surface over which an optical disturbance has a constant phase" (Hecht and Zajac, 1974). The route taken will be the smallest Optical Path Length (OPL) according to Fermat's Principle. The OPL is expressed mathematically as:

$$OPL = \int_{S}^{P} n(s) \ ds \ , \tag{A5}$$

where n is the index of refraction (the ratio of the speed of an EM wave in vacuum to that in matter), s is the path length, and S and P represent the end points of the shortest light path. The

propagating wave's phase is k = 2π/λ * OPL. Phase distortions occur when a wavefront encounters random irregularities in the atmosphere's index of refraction. Such irregularities are due to atmospheric turbulent mixing processes. To approximate the atmospheric random irregularities, statistical quantities need to be utilized. However, they are not always single valued, unique or even bounded. Kolomogorov and Tatarski developed the concept of structure functions and local homogeneity to resolve this hurdle. Without digging into an extensive theoretical discussion, the structure function for an arbitrary spatially distributed random variable as defined by Kolmogorov and Tatarski (Tatarski, 1961; Stull, 1988) is:

$$D_R(\bar{r}) = <[R(\bar{r}_1)\text{-}R(\bar{r}_2)]^2>, \tag{A6}$$

where R is homogeneous and isotropic. Applying this formula to the index of refraction,

$$C_n^2 = \frac{<(n_1\text{-}n_2)^2>}{r^{2/3}}, \tag{A7}$$

where r is the distance between two sample points, and between the turbulence inner-scale and turbulence outer-scale. Note: At scales smaller than the inner-scale, eddy energy dissipates through viscous effects. The outer-scale represents the "largest scale size for which eddies may be considered isotropic" (Clifford, 1978).

As defined in Tatarski's 1961 publication, the index of refraction is a function of pressure and temperature:

$$n\text{-}1 = (79\times10^{-6}) * \frac{P}{T}. \tag{A8}$$

Combining these last two equations, one can use the temperature structure parameter:

$$C_T^2 = \frac{<(T_1\text{-}T_2)^2>}{r^{2/3}}, \tag{A9}$$

to calculate the C_n^2. The end result is:

$$C_n^2 = (79\times10^{-6}\frac{P}{T})^2 * C_T^2, \tag{A10}$$

Thus we see the quantifiable AOT parameter C_n^2, as a function of pressure and temperature.

A-4.2   Relating Index of Refraction to Temperature

Light traveling through the atmosphere will bend in the direction of the denser atmosphere. Cold air is denser than warm air, having a greater index of refraction. Thus, light will bend toward the cold air. In the context of the surface layer, if the air at the surface is warmer than the air above,

the light ray bends in a concave, upward trajectory. An example of this concept is witnessed when one views a mirage along a distant horizon. Snell's Law (http://en.wikipedia.org/wiki/Snell's_law, 2009 February 13) demonstrates the relationship between the incident/reflective angles and the index of refraction:

$$n_1 \sin \theta_1 = n_2 \sin \theta_2, \qquad \text{(A11)}$$

where this θ is the angle of incidence and refraction, and n is the index of refraction.

Within the atmosphere's ever-changing surface layer, there are numerous density variations that occur as a function of the solar heating and radiative cooling. To quantify the atmospheric density variations is very difficult, for several reasons. First, the random nature of the variations requires a statistical approach such as was described in section A-4.1. Second, there are no commonly accessible density measurement devices. There are, however, commonly accessible temperature measurement devices and a correlation between atmospheric density and temperature. The complex relationship shown in A-4.1 can be simplified (for concept purposes) to the following:

One of the more well known equations relating density with temperature is the Ideal Gas Law:

$$P = \rho RT , \qquad \text{(A12)}$$

where P is pressure, ρ is density, R is the universal gas constant and T is temperature.

Isolating density (ρ), one can see that density is inversely proportional to temperature:

$$\rho = \frac{P}{RT} , \qquad \text{(A13)}$$

Thus, when density increases, temperature decreases. In terms of gradient temperatures, we know from the mirage example that when light encounters a colder, denser environment, that light will systematically 'bend' toward the cold environment. Extend this gross concept along a path of warm and cold air pockets near the surface and one can more easily envision a very random light path; one that needs a statistical parameter such as a structure function to quantify.

A-5 Correlating AOT and ΔT

We know that stability, atmospheric density, vertical temperature gradients and turbulent parameters are related. Therefore, it is not surprising that vertical temperature gradients sampled along the same volume of air through which AOT is measured (C_n^2) are systematically correlated.

The following observations are taken from an operational test environment, where AOT (C_n^2) and ΔT have been routinely quantified. When a C_n^2 time series is overlaid with a ΔT time series, an interesting pattern is observed. The following table summarizes these observations:

C_n^2	ΔT	Vertical Profile	Buoyancy	Stability State
Minimum	Near 0^oC	Isothermal	Equilibrium	Neutral Event
Maximum	$< 0^oC$	T decreases with height	Positively Buoyant	Unstable
	$> 0^oC$	T increases with height	Negatively Buoyant	Stable

When C_n^2 goes to a minimum, then ΔT reports a value at or near $0\ ^oC$. This near-isothermal condition is called a "neutral event." When the ΔT reports a negative value, C_n^2 shows more turbulence. Often the maximum C_n^2 is associated with very negative ΔT values. When the ΔT reports a positive value, C_n^2 reports less turbulence present. For an example of the stability states in a 24-h C_n^2 cycle, see Vaucher and Endlich (1994).

List of Symbols, Abbreviations, and Acronyms

ΔT   Delta Temperature

ρ   density

3DWF   3-Dimensional Wind Field

AOT   atmospheric optical turbulence

ARL   Army Research Laboratory

C   Celsius

EO   electro-optical

JD   Julian Date

LT   local time (mountain time)

NE   Neutral Event

OPL   Optical Path Length

P   pressure

R   universal gas constant for dry air

T   temperature

UHI   Urban Heat Island

W03US   *WSMR 2003 Urban Study*

W05US   *WSMR 2005 Urban Study*

W07US   *WSMR 2007 Urban Study*

WSMR   White Sands Missile Range

No. of Copies	Organization
1 PDF	ADMNSTR DEFNS TECHL INFO CTR DTIC OCP 8725 JOHN J KINGMAN RD STE 0944 FT BELVOIR VA 22060-6218
3 HCs	US ARMY RSRCH LAB ATTN RDRL CIM P TECHL PUB ATTN RDRL CIM L TECHL LIB ATTN IMNE ALC HRR MAIL & RECORDS MGMT 2800 POWDER MILL ROAD ADELPHI MD 20783-1197
1 CD	US ARMY RSRCH LAB ATTN RDRL CIM G TECHL LIB T LANDFRIED APG MD 21005-5066
10 CD 10 HCS	US ARMY RSRCH LAB G VAUCHER ATTN RDRL CIE D BLD 1622 WSMR NM 88002

Total: 25 (1 PDF, 11 CDs, 13 HCs)

INTENTIONALLY LEFT BLANK.